
Topological Methods for fMRI Data

Bastian Rieck^{*12} Tristan Yates^{*3} Christian Bock¹² Karsten Borgwardt¹² Guy Wolf⁴⁵
Nicholas Turk-Browne^{†3} Smita Krishnaswamy^{†67}

Abstract

Functional magnetic resonance imaging (fMRI) is a crucial technology for gaining insights into cognitive processes in humans. Data amassed from fMRI measurements result in volumetric data sets that vary over time. However, analysing such data presents a challenge due to the large degree of noise, and person-to-person variation in how information is represented in the brain. To address this challenge, we present a novel topological approach that encodes each time point in an fMRI data set as a persistence diagram of topological features, i.e. high-dimensional voids present in the data. This representation naturally does not rely on voxel-by-voxel correspondence and is robust towards noise. We show that these time-varying persistence diagrams can be clustered to find meaningful groupings between participants, and that they are also useful in studying within-subject brain state trajectories as each subject is performing a task, for example. Here, we apply both clustering and trajectory analysis techniques to a group of participants watching the movie ‘Partly Cloudy’. We note that there are marked differences in both brain state trajectories and overall topological features between adults and children watching the same movie.

1. Introduction

Human cognitive processes are commonly studied using functional magnetic resonance imaging (fMRI), amassing highly complex, well-structured, and time-varying data sets across multiple individual subjects. The ultimate goal of extracting higher-level abstractions from such data is primarily impeded by two factors: (i) the measurements are inherently noisy, due to changes in machine calibration, spurious patient movements, and environmental conditions, (ii) there is a high degree of variability even between otherwise healthy brains (e.g. in terms of the representation of stimulus and activity in the brain).

While these factors can be mitigated by certain experimental protocols and preprocessing decisions, they cannot be eliminated. This demonstrates the need for using representations that are to some extent *robust* with respect to noise and *invariant* with respect to isometric transformations in order to better capture cognitively-relevant fMRI activity, particularly across populations where anatomy-function relations may differ. In this paper, we present a novel topological approach that can study time-varying fMRI data in the form of cubical complexes. Our approach is coordinate-free, thus inherently providing a stable representation of high-level brain activity. We note that this approach is inherently different from many approaches for fMRI data in that it does not require the creation of a correlation graph, and operates on the raw activations themselves.

2. Related work

Cubical complexes—our main data structure for modelling an fMRI data set—and their homology are already well-studied in algebraic topology, but their use in real-world applications was primarily limited to image segmentation (Allili et al., 2001) for a long time. This changed with the rise of persistent homology, which also gave rise to research that extends this concept to the cubical setting, either *directly* (Strömbom, 2007; Wagner et al., 2012) or *indirectly* (Nanda, 2012), such that the properties of ‘cubical persistent homology’ are well-studied (Dłotko & Wanner, 2018; Mrozek & Wanner, 2010; Wang & Wei, 2016). Moreover, there is some previous work fusing fMRI analysis and topological data analysis, but it is either based on auxiliary

^{*}Equal contribution. [†]These authors jointly directed this work. ¹Department of Biosystems Science and Engineering, ETH Zurich, Switzerland ²SIB Swiss Institute of Bioinformatics, Switzerland ³Department of Psychology, Yale University, New Haven, CT, USA ⁴Department of Mathematics & Statistics, Université de Montréal, Montréal, QC, Canada ⁵Mila – Quebec AI Institute, Montréal, QC, Canada ⁶Department of Computer Science, Yale University, New Haven, CT, USA ⁷Department of Genetics, Yale University, New Haven, CT, USA. Correspondence to: Bastian Rieck <bastian.rieck@bsse.ethz.ch>, Nicholas Turk-Browne <nicholas.turk-browne@yale.edu>, Smita Krishnaswamy <smita.krishnaswamy@yale.edu>.

topological representations (Saggar et al., 2018), such as the MAPPER algorithm (Singh et al., 2007), or it makes use of functional connectivity information, requiring the extraction of regions of interest (Anderson et al., 2018). By contrast, our method operates *directly* on fMRI volumes, requiring neither additional location information nor the construction of auxiliary representations (our method benefits from using whole-brain masks, yet they are not a prerequisite for the analyses described in this paper).

3. Background

Topological data analysis (TDA) recently started gaining traction, in particular in the context of machine learning; see Hofer et al. (2017) or Rieck et al. (2019) for two recent examples¹. TDA is a rapidly-growing field that provides tools for analysing the shape of data sets. It is deeply rooted within algebraic topology and uses numerous of its concepts. This section provides a brief introduction, we refer the reader to Edelsbrunner & Harer (2010) for details. To our knowledge, this is the first time that such a *direct* topological analysis has been applied to fMRI data.

Simplicial homology. The central object in algebraic topology is a simplicial complex K , i.e. a high-dimensional generalisation of a graph. It is commonly used to describe complex objects such as manifolds (we deviate from this notion but follow the conventional exposition, which focuses primarily on a simplicial view). The connectivity of K is analysed by means of simplicial homology, a framework employing matrix reduction algorithms similar to Gaussian elimination in order to assign K a graded set of groups, the homology groups. Homology groups provide a description of the topological features of K . For low dimensions d , these features afford an intuitive description and are called *connected components* ($d = 0$), *tunnels* ($d = 1$), and *voids* ($d = 2$), respectively. The number of d -dimensional topological features is referred to as the d th Betti number $\beta_d \in \mathbb{N}$; it is used to distinguish between different topological objects: for example, a circle—the boundary of a disk—has Betti numbers $(1, 1)$, while a filled square has Betti numbers $(1, 0)$.

Persistent homology. The analysis of real-world data sets using topological methods requires addressing two limiting factors: first, real-world data sets are typically unstructured and require topological approximations². Second, the ‘static’ topology of real-world data sets is often insufficient and one is more interested in analysing the behaviour of a *function*

over a data set. Betti numbers are of limited use here because they can only represent simple counts. However, endowed with additional information, they can be used as multi-scale topological descriptors. This is the motivation of *persistent homology*, an extension of simplicial homology to scenarios in which a simplicial complex K and an additional function $f: K \rightarrow \mathbb{R}$ exists. Assuming that f can only attain a finite set of function values $f_0 \leq f_1 \leq \dots \leq \dots \leq f_{m-1} \leq f_m$, it is possible to sort K according to f , leading to a nested sequence of simplicial complexes

$$\emptyset = K_0 \subseteq K_1 \subseteq \dots \subseteq K_{m-1} \subseteq K_m = K, \quad (1)$$

which is referred to as a *filtration*, with $K_i := \{\sigma \in K \mid f(\sigma) \leq f_i\}$, i.e. each subset contains only those simplices whose function value is less than or equal to the threshold. A filtration can be seen as representing the ‘evolution’ of K along the function. Similar to the Watershed transform in image processing (Roerdink & Meijster, 2000), topological features are *created* (a new connected component might arise) and *destroyed* (two connected components might merge into one) over the course of a filtration. Persistent homology is capable of tracking the evolution of topological features and represents each feature as a tuple of its creation and destruction value $(f_i, f_j) \in \mathbb{R}^2$, with $i \leq j$ and $f_i, f_j \in \text{im}(f)$.

Persistence diagrams. The tuples generated by persistent homology are collated according to their dimension d and stored in the d th *persistence diagram* \mathcal{D}_d . This diagram essentially summarises all topological activity in dimension d . As a consequence of the calculation process, all points in \mathcal{D}_d are situated *above* the diagonal³. The quantity $\text{pers}(x, y) := |y - x|$ of a point $(x, y) \in \mathcal{D}_d$ is called the *persistence* of its corresponding topological feature. Low-persistence features are usually considered to be ‘noise’, while high-persistence features are taken to correspond to ‘real’ features of a data set (Edelsbrunner et al., 2002). Recent work cast some doubts as to whether this assumption is always justified (Bendich et al., 2016); in particular for clinical data, low persistence merely implies ‘low reliability’, *not* necessarily ‘low importance’.

4. Methods

In the following, we will be dealing with time-varying fMRI, i.e. we are observing an activation function $f: \mathcal{V} \times \mathcal{T} \rightarrow \mathbb{R}$ over a 3D bounded volume $\mathcal{V} \subset \mathbb{R}^3$ and a set of time steps \mathcal{T} . For $t \in \mathcal{T}$, the function $f(\cdot, t)$ is typically visualised using either stacks of images (Figure 1a) or volume rendering (Figure 1b). While it would be possible to analyse individual images, we opt for transforming \mathcal{V} into a

¹There are more TDA publications, but the aforementioned ones focus on graph classification, which is related to our scenario.

²The standard procedure involves calculating a neighbourhood graph and expanding it into a simplicial complex. It will *not* be required in our case.

³It is also possible to reverse the order of the filtration, leading to all points being situated *below* the diagonal.

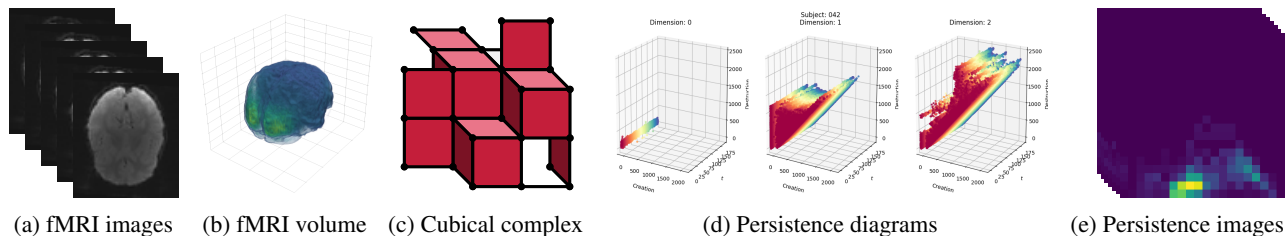


Figure 1. A graphical overview of our method. We represent an fMRI stack (a) as a volume (b), from which we create a sequence of cubical complexes (c). Calculating the persistent homology of the sequence of cubical complexes results in a set of time-varying persistence diagrams (d) for dimensions 0, 1, and 2. We calculate summary statistics from the sequence of diagrams (not shown), and convert them to vectorial representations (e) for downstream processing tasks (only the sequence for a single dimension is depicted here).

cubical complex C , i.e. an equivalent of a simplicial complex, in which the triangles and tetrahedra (and their higher-dimensional generalisations) have been replaced by squares and cubes. In contrast to simplicial complexes, cubical complexes are perfectly suited to represent an fMRI volume \mathcal{V} because each voxel corresponds precisely to one cubical simplex (whereas if we were to use a simplicial complex to model \mathcal{V} , we would have to employ interpolation schemes as there is no natural mapping from voxels to tetrahedra).

Terminology. We assume that we are given a data set of n volumes $\mathcal{V}_1, \dots, \mathcal{V}_n$ of the same dimensions, corresponding to n different individuals, and a set of m time steps $\mathcal{T} = \{t_1, \dots, t_m\}$. We use f_i to denote the activation function of the i th volume, i.e. $f_i: \mathcal{V}_i \times \mathcal{T} \rightarrow \mathbb{R}$. Here, the activation functions are *aligned* with respect to their time steps; this is a simplifying assumption that simplifies the subsequent analysis steps and does not impose a restriction in practice.

Computing topological features. We calculate the topological features of f_i using the following steps: (1) Convert the volume \mathcal{V}_i to a cubical complex C_i . (2) For each time step t_j , assign the values of $f_i(\cdot, t_j)$ to C_i . (3) Calculate persistent homology of the filtration according to Equation 1 and collate the resulting set of persistence diagrams. Each participant is assigned persistence diagrams in dimensions 0, 1, and 2. Since each \mathcal{V}_i is three-dimensional, higher-dimensional persistence diagrams are empty and we do not have to consider them. We can plot the resulting persistence diagrams of each participant as a set of points in \mathbb{R}^3 , with the additional axis being used to represent *time* (Figure 1d).

4.1. fMRI dataset

We evaluate our topological approach using open-source fMRI data (Richardson et al., 2018), available on the OpenNeuro database (accession number ds000228). Participants were 33 adults (18–39 years old; $M = 24.8$, $SD = 5.3$; 20 female) and 122 children (3.5–12 years old; $M = 6.7$, $SD = 2.3$; 64 female) who watched the same animated movie (Sohn & Reher, 2009) while undergoing

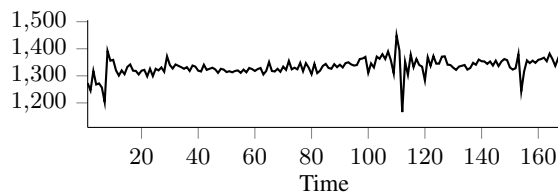


Figure 2. Example of a summary statistics curve, based on the infinity norm of a persistence diagram, for one of the participants.

fMRI (gradient-echo EPI sequence: $TR = 2$ s, $TE = 30$ ms, flip angle = 90° , matrix = 64×64 , slices = 32, interleaved slice acquisition). Data were collected using the standard Siemens 32-channel head coil for adults and older children. One of two custom 32-channel phased-array head coils was used for younger children (smallest coil: $N = 3$; $M = 3.91$, $SD = 0.42$ years old; smaller coil: $N = 28$; $M = 4.07$, $SD = 0.42$, years old). Acquisition parameters differed slightly across participants but all fMRI data were resampled to have the same voxel size: 3 mm isotropic with 10% slice gap. A T1-weighted structural image was also collected for all subjects (MPRAGE sequence: GRAPPA = 3, slices = 176, resolution = 1 mm isotropic, adult coil FOV = 256 mm, child coils FOV = 192 mm). Imaging data were pre-processed using fMRIPrep v1.1.8 (Esteban et al., 2019). A full description of the pre-processing can be found in another study using this dataset (Yates et al., 2020). The relevant outputs of this pipeline are: a 4-dimensional (x -coordinate by y -coordinate by z -coordinate by time) fMRI time series and a whole-brain mask for each individual subject. The fMRI time series includes 162 2 s time steps that correspond to the same point in the movie for each subject.

4.2. Global analysis based on summary statistics

Extracting information from the time-varying persistence diagrams of each participant is impeded by their complex geometrical structure. We first focus on a description of *global* properties of participants, restricting ourselves to persistence diagrams with $d = 2$. To this end, we calculate topological summary statistics, such that the sequence

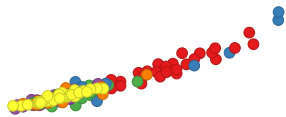


Figure 3. An embedding of the distances between topological summaries, colour-coded by the subject age group.

of diagrams for the i th participant becomes scalar-valued time-series. We primarily focus on one summary statistic here (the results that we obtain with *total persistence*—another summary statistic—are virtually identical, so we omitted them), i.e. the *infinity norm* $\|\mathcal{D}\|_\infty$ of a persistence diagram (Cohen-Steiner et al., 2007), defined by

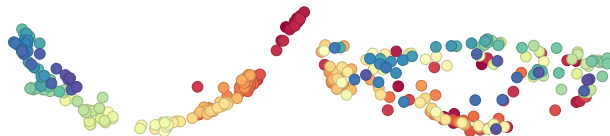
$$\|\mathcal{D}\|_\infty := \max_{x,y \in \mathcal{D}} \text{pers}(x,y)^p, \quad (2)$$

with $p \in \mathbb{R}$. We found $p = 1$ to be sufficient (implying that we use the original persistence values). Since Equation 2 results in scalar values, it turns a sequence of persistence diagrams into a time series. Figure 2 depicts this for a single participant. Letting $\mathcal{C}^{(i)}$ refer to the time series ‘curve’ of participant i , we can cluster different curves by calculating the Euclidean distance between their curve representations. Using hierarchical clustering (Hastie et al., 2009, pp. 520–528), we thus obtain a clustering solely based on summary topological information.

Evaluation. The clustering is capable of discovering a split between two groups tightly associated with the participants’ age, even though our topological feature extraction pipeline is unaware of these groups *a priori*. A binary clustering shows high alignment scores with those two groups: the *adjusted Rand index* (Hubert & Arabie, 1985) of the partition is 0.74 (where 1.0 would indicate perfect agreement up to permutation), while the *adjusted mutual information score* (Vinh et al., 2010) is 0.58 (again, 1.0 would indicate perfect agreement). Both indices are adjusted for chance, i.e. a value of 0.0 would indicate that the clustering is essentially random. This alignment demonstrates that there are topological differences in the way different age groups process the movie; we plan on further studying them in future work. On the qualitative level, a visualisation of the distance between the topological summaries (Figure 3) shows that the variability within one age group (red points; after performing the analysis, the labels were uncovered and are seen to correspond to the *adult* participants in the study) is clearly larger than for the remaining ones. ‘Disentangling’ the remaining groups will require a more sensitive analysis.

4.3. Local analysis based on brain state trajectories

The global analysis is useful to obtain summary information about the data set and observe overall groupings. We can also use topological information to visualise (and analyse)



(a) High temporal coherence (b) Low temporal coherence

Figure 4. Brain state trajectories of two participants based on a persistence image representation. Each point represents an individual time step; the colour correspond to time (moving from red to blue as time progresses).

the status of each participant during an experiment. This necessitates being able to define distances or dissimilarities between persistence diagrams. Since metrics between persistence diagrams have a high computational complexity (Kerber et al., 2017), we sidestep this issue and use *persistence images* (Adams et al., 2017), a method for using density estimation to convert a persistence diagram into an ‘image’ of fixed dimensions (Figure 1e). Thus, we transform the persistence diagrams of the i th participant into a matrix $\mathbf{X}^{(i)} \in \mathbb{R}^{m \times r^2}$, where the j th row corresponds to the ‘unravalled’ persistence diagram of time step t_j . We use PHATE (Moon et al., 2019), a powerful embedding algorithm for time-varying data, to represent $\mathbf{X}^{(i)}$ as a lower-dimensional trajectory. This trajectory represents the state of the brain, measured using topological features, so we refer to it as the *brain state trajectory*. Figure 4 depicts example trajectories. We assess the *temporal coherence* of each trajectory, i.e. to what extent the trajectory revisits previous time steps, by counting the fraction of how many of the $k = 3$ nearest neighbours of each point are more than $t = 3$ time steps removed from it, and then calculating the average score over the length of a trajectory. According to this measure, the coherence of one of the participant groups is on average *higher* than those of the other groups ($M = 47.31$, $SD = 5.31$ vs. $M = 42.30$, $SD = 3.93$; upon uncovering the labels, these participants turned out to comprise the *youngest* participants). Hence, this group appears to give rise to temporally-coherent brain state trajectories (Figure 4a), hinting at differences in brain states between participant groups.

5. Conclusion

This paper demonstrates the potential of topology-based feature extraction for fMRI data to permit analyses on both the global and the local level. In the future, we want to analyse brain state trajectories and link states *back* to ‘events’ in the task, such as the appearance of a character in a movie. Moreover, we plan on investigating to what extent topological features can be useful to predict or ‘learn’ information about participants, including their age group or certain behavioural scores, for example.

References

- Adams, H., Emerson, T., Kirby, M., Neville, R., Peterson, C., Shipman, P., Chepushtanova, S., Hanson, E., Motta, F., and Ziegelmeier, L. Persistence images: A stable vector representation of persistent homology. *Journal of Machine Learning Research*, 18(8):1–35, 2017.
- Allili, M., Mischaikow, K., and Tannenbaum, A. Cubical homology and the topological classification of 2D and 3D imagery. In *Proceedings of the IEEE International Conference on Image Processing*, volume 2, pp. 173–176, 2001.
- Anderson, K. L., Anderson, J. S., Palande, S., and Wang, B. Topological data analysis of functional MRI connectivity in time and space domains. In *Connectomics in NeuroImaging*, 2018.
- Bendich, P., Marron, J. S., Miller, E., Pieloch, A., and Skwerer, S. Persistent homology analysis of brain artery trees. *Annals of Applied Statistics*, 10(1):198–218, 2016.
- Cohen-Steiner, D., Edelsbrunner, H., and Harer, J. Stability of persistence diagrams. *Discrete & Computational Geometry*, 37(1):103–120, 2007.
- Dłotko, P. and Wanner, T. Rigorous cubical approximation and persistent homology of continuous functions. *Computers & Mathematics with Applications*, 75(5):1648–1666, 2018.
- Edelsbrunner, H. and Harer, J. *Computational topology: An introduction*. Providence, RI, USA, 2010.
- Edelsbrunner, H., Letscher, D., and Zomorodian, A. J. Topological persistence and simplification. *Discrete & Computational Geometry*, 28(4):511–533, 2002.
- Esteban, O., Markiewicz, C. J., Blair, R. W., Moodie, C. A., Isik, A. I., Erramuzpe, A., Kent, J. D., Goncalves, M., DuPre, E., Snyder, M., Oya, H., Ghosh, S. S., Wright, J., Durnez, J., Poldrack, R. A., and Gorgolewski, K. J. fMRIPrep: a robust preprocessing pipeline for functional MRI. *Nature Methods*, 16(1):111–116, 2019.
- Hastie, T., Tibshirani, R., and Friedman, J. *The Elements of Statistical Learning*. Second edition, 2009.
- Hofer, C., Kwitt, R., Niethammer, M., and Uhl, A. Deep learning with topological signatures. In Guyon, I., Luxburg, U. V., Bengio, S., Wallach, H., Fergus, R., Vishwanathan, S., and Garnett, R. (eds.), *Advances in Neural Information Processing Systems 30*, pp. 1634–1644. Curran Associates, Inc., 2017.
- Hubert, L. and Arabie, P. Comparing partitions. *Journal of Classification*, 2(1):193–218, 1985.
- Kerber, M., Morozov, D., and Nigmatov, A. Geometry helps to compare persistence diagrams. *Journal of Experimental Algorithmics*, 22, 2017.
- Moon, K. R., van Dijk, D., Wang, Z., Gigante, S., Burkhardt, D. B., Chen, W. S., Yim, K., Elzen, A. v. d., Hirn, M. J., Coifman, R. R., Ivanova, N. B., Wolf, G., and Krishnaswamy, S. Visualizing structure and transitions in high-dimensional biological data. *Nature Biotechnology*, 37(12):1482–1492, 2019.
- Mrozek, M. and Wanner, T. Coreduction homology algorithm for inclusions and persistent homology. *Computers & Mathematics with Applications*, 60(10):2812–2833, 2010.
- Nanda, V. *Discrete Morse Theory For Filtrations*. PhD thesis, Rutgers University, 2012.
- Richardson, H., Lisandrelli, G., Riobueno-Naylor, A., and Saxe, R. Development of the social brain from age three to twelve years. *Nature Communications*, 9(1):1–12, 2018.
- Rieck, B., Bock, C., and Borgwardt, K. A persistent Weisfeiler–Lehman procedure for graph classification. In Chaudhuri, K. and Salakhutdinov, R. (eds.), *Proceedings of the 36th International Conference on Machine Learning*, volume 97 of *Proceedings of Machine Learning Research*, pp. 5448–5458. PMLR, 2019.
- Roerdink, J. B. T. M. and Meijster, A. The watershed transform: Definitions, algorithms and parallelization strategies. *Fundamenta Informaticae*, 41:187–228, 2000.
- Saggar, M., Sporns, O., Gonzalez-Castillo, J., Bandettini, P. A., Carlsson, G., Glover, G., and Reiss, A. L. Towards a new approach to reveal dynamical organization of the brain using topological data analysis. *Nature Communications*, 9(1):1399, 2018.
- Singh, G., Mémoli, F., and Carlsson, G. Topological methods for the analysis of high dimensional data sets and 3D object recognition. In *Eurographics Symposium on Point-Based Graphics*, 2007.
- Sohn, P. and Reher, K. Partly cloudy [motion picture], 2009. Pixar Animation Studios and Walt Disney Pictures.
- Strömbom, D. Persistent homology in the cubical setting: Theory, implementations and applications. Master’s thesis, Luleå University of Technology, 2007.
- Vinh, N. X., Epps, J., and Bailey, J. Information theoretic measures for clusterings comparison: Variants, properties, normalization and correction for chance. *Journal of Machine Learning Research*, 11(95):2837–2854, 2010.

Wagner, H., Chen, C., and Vuçini, E. Efficient computation of persistent homology for cubical data. In *Topological Methods in Data Analysis and Visualization II: Theory, Algorithms, and Applications*, pp. 91–106. 2012.

Wang, B. and Wei, G.-W. Object-oriented persistent homology. *Journal of Computational Physics*, 305:276–299, 2016.

Yates, T. S., Ellis, C. T., and Turk-Browne, N. B. Emergence and organization of adult brain function throughout child development. *bioRxiv*, 2020. doi: 10.1101/2020.05.09.085860.